

RESEARCH ARTICLE

Open Access



Synthesis, structure and toxicity evaluation of ethanolamine nitro/chloronitrobenzoates: a combined experimental and theoretical study

Manuela Crisan¹, Liliana Halip¹, Paulina Bourosh², Sergiu Adrian Chicu³ and Yurii Chumakov^{2*}

Abstract

Background: Nitroaromatic and chloronitroaromatic compounds have been a subject of great interest in industry and recently in medical-pharmaceutical field. 2-Chloro-4-nitro/2-chloro-5-nitrobenzoic acids and 4-nitrobenzoic acid are promising new agents for the treatment of main infectious killing diseases in the world: immunodeficiency diseases and tuberculosis.

Results: New ethanolamine nitro/chloronitrobenzoates were synthesized and characterized by X-ray crystallography, UV-vis, FT-IR and elementary analysis techniques. The toxicity of the compounds prepared and correspondent components was evaluated using *Hydractinia echinata* as test system. A significant lower toxicity was observed for nitro-derivative compared with chloronitro-derivatives and individual components. Crystallographic studies, together with the chemical reactivity and stability profiles resulted from density functional theory and ab initio molecular orbital calculations, explain the particular behavior of ethanolamine 4-nitrobenzoate in biological test.

Conclusions: The experimental and theoretical data reveal the potential of these compounds to contribute to the design of new active pharmaceutical ingredients with lower toxicity.

Keywords: Nitrobenzoic and chloronitrobenzoic acids and derivatives, Toxicity, Single crystal X-ray diffraction, Chemical reactivity

Introduction

Nitroaromatic and chloronitroaromatic compounds are versatile precursors, the vast majority synthetic and frequently employed as important intermediates for the synthesis of industrial chemicals, dyes, pigments and pharmaceutical drugs [1–3]. The functional groups nitro and chloride provide chemical and structural diversity and a significant impact on properties and reactivities of chemicals, making these compounds attractive in different research fields over the past decades. Many pharmaceuticals have their chemical origins in nitro- and chloronitroaromatic compounds. They are used to treat

a wide variety of diseases categories: Parkinson, angina, insomnia and parasitic infection (e.g. *Giardiasis*, *Amebiasis*, *Trichomoniasis*) [4–6]. Recently, 4-nitrobenzoic acid (4-NO₂BA), 2-chloro-4-nitrobenzoic acid (2-Cl-4-NO₂BA) and 2-chloro-5-nitrobenzoic acid (2-Cl-5-NO₂BA) have been used as active ingredients in the main infectious killing diseases in the world. Therefore, 4-NO₂BA is used as inhibitor agent for identification of *Mycobacterium tuberculosis* complex [7–9] and 2-Cl-4-NO₂BA/2-Cl-5-NO₂BA used in a novel therapy for immunodeficiency diseases, including the human immunodeficiency virus (HIV) infection [10, 11].

Taking into account the prospects of nitro- and chloronitrobenzoic acids and the fact that about a half of all active pharmaceutical ingredients are used today as salts due to their improved drug's physicochemical properties,

*Correspondence: chumakov@phys.asm.md

² Institute of Applied Physics, Academy of Sciences of Moldova, Academiei Street 5, 2028 Chisinau, Republic of Moldova
Full list of author information is available at the end of the article

we have focused to prepare new nitro/chloronitroderivatives with lower toxicity. Limited information on the experimental toxicity profile of benzoic agents have been founded in literature [12–15]. Experimental and/or theoretical toxicity studies on different organisms are required for new derivatives of an active pharmacological substance. The safety profile of a salt depends significantly on the cation nature and the alkyl side chain. The majority of hydrogen-bonded complexes of nitro-, respectively chloronitrobenzoic acids use heterocyclic amines (e.g. pyridine, piperazine, morpholine), considered strong mutagens [16–18].

This study proposes the development of new compounds with dual biological activity, based on biologically active components: ethanolammonium as cation and 2-chloro-4-nitrobenzoate, 2-chloro-5-nitrobenzoate and respectively 4-nitrobenzoate as anions. Ethanolamine (EA) is a naturally occurring component and a suitable model of alkanolamines, which is safer, economical and commercially available, used as base chemical in the production of pharmaceuticals. It is an essential component of cell membranes, present in the synthesis of membrane lipids, such as phosphatidylethanolamine and phosphatidylcholine [19]. Recent studies introduce EA as a new therapeutic agent in the treatment of age-associated human diseases, being involved in autophagy regulation [20].

Besides the plethora of properties noted above, both EA and substituted benzoic acids have the ability to establish strong and directional hydrogen bonds, forming supramolecular systems with different topologies, important in crystal engineering [21–23]. Continuing our interest in multicomponent organic crystal with dual biological activity, some of the major objectives of this paper are to obtain crystalline ethanolamine salts of 2-Cl-4-NO₂BA (1), 2-Cl-5-NO₂BA (2) and 4-NO₂BA (3), to characterize them physico-chemically and structurally, and to investigate their supramolecular synthons and molecular packing. A comparative analysis on toxicity of the compounds studied is also presented, using *Hydractinia echinata*, previously demonstrated to be an excellent test system [12, 24]. In order to explain the particular behavior of ethanolamine salts of nitro- and chloronitrobenzoic acids in biological test, a theoretical study regarding the chemical reactivity and stability profiles was described in correlation with their biological activity (toxicity) and X-ray structures.

Experimental

General

All the chemicals used for the synthesis were of analytical grade and purchased from Fluka AG (Buchs SG). EA was freshly distilled before any use. Melting points were

determined on Boetius melting point apparatus and are uncorrected. FT-IR spectra of new synthesized compounds were recorded as KBr pellet on a JASCO—FT/IR-4200 spectrometer, in the range 4000–400 cm⁻¹, with a resolution of 4.0 cm⁻¹ and a scanning speed of 16 mm s⁻¹. The optical properties were examined by using a UV–vis spectrophotometer at room temperature. UV–vis spectra in the 190–800 nm range were measured on PERKIN-ELMER LAMBDA 12 UV–vis spectrometer.

Synthesis and characterization of compounds 1–3

Title compounds were prepared in a 1:1 molar ratio via proton exchange reaction by mixing the diethyl ether solutions of ethanolamine and 2-Cl-4-NO₂BA/2-Cl-5-NO₂BA, respectively 4-NO₂BA. The mixture was stirred and heated to reflux for 30 min to complete the reaction. The yellowish solutions obtained were kept for slow evaporation. After a few days, crystals suitable for X-ray diffraction were obtained. The crystals were filtered and washed with diethyl ether and dried in air. The reaction yields were about 90–92%. The purity of the obtained compounds ranged between 99.1 and 99.4%, established by an UV spectrophotometric method [25] and confirmed by elemental analysis. The FT-IR spectra for each compound were consistent with salt formation.

1. C₉H₁₂ClN₂O₅ (262.58), m.p. 112–115 °C; λ_{max} = 277.93 nm; FT-IR spectra (KBr pelet, cm⁻¹): 3194 (νNH₃⁺), 1613 (ν_{as}COO⁻), 1520 (δNH₃⁺), 1394 (ν_sCOO⁻), 1065 (νC–O), calcd. (%): C 41.13, H 4.57, Cl 13.52, N 10.66; found (%): C 41.04, H 4.41, Cl 13.39, N 10.51;
2. C₉H₁₂ClN₂O₅·H₂O (280.58), m.p. 116–118 °C; λ_{max} = 279.81 nm; FT-IR spectra (KBr pelet, cm⁻¹): 3166 (νNH₃⁺), 1621 (ν_{as}COO⁻), 1519 (δNH₃⁺), 1404 (ν_sCOO⁻), 1087 (νC–O), calcd. (%): C 38.49, H 4.99, Cl 12.65, N 9.98; found (%): C 38.39, H 4.82, Cl 12.48, N 9.84;
3. C₉H₁₂N₂O₅ (228.20), m.p. 173–175 °C; λ_{max} = 273.55 nm; FT-IR spectra (KBr pelet, cm⁻¹): 2955 (νNH₃⁺), 1648 (ν_{as}COO⁻), 1515 (δNH₃⁺), 1392 (ν_sCOO⁻), 1018 (νC–O), calcd. (%): C 47.33, H 5.25, N 12.27; found (%): C 47.18, H 5.13, N 12.09;

Single crystal X-ray structure analysis

The X-ray data sets were collected at room temperature on a Siemens P3/PC diffractometer equipped with CuKα-radiation. The unit cell parameters were determined, and the structures refinement were performed using the SHELX-97 program [26]. Non hydrogen atoms have been refined with anisotropic displacement. Hydrogen atoms were found from differential Fourier maps and refined without any constraints. Hydrogen atoms that are

not involved in hydrogen bonding were omitted from the representation of crystal packings. The crystals remained stable throughout the data collection. Drawings of the structures of 1–3 compounds were produced using ORTEP program (Fig. 1) [27].

Crystallographic data and refinement for compounds 1–3 were summarized in Table 1.

Crystallographic data were deposited in the Cambridge Crystallographic Data Centre (CCDC Numbers 853484, 853485, 257807).

Toxicity test

The toxicity of compounds 1–3 and the correspondent components was evaluated using *H. echinata* as test system. This simple and common invertebrate living in European and North American coastal areas is rapidly reproducible and considered sustainable for in vivo experiments. The used method was identical with the one described in previous articles [12, 24]. Dishes with 30 *H. echinata* larvae were exposed to 3 mL seawater (980 mosmol, pH 8.2, 18 °C) containing 20 mM CsCl and the test compounds were added for 3 h. The concentration (mol L⁻¹) at which the frequency of metamorphosis induction larvae to polyp was reduced by 50% with respect to control was determined after 24 h and noted as MRC₅₀ (metamorphosis reducing concentration) and correspond to EC₅₀ (50-effective concentration) in literature. The measured value of toxicity (M) was showed as logarithm of reciprocal value of MRC₅₀ ($M = \log 1/\text{MRC}_{50}$). Triplicate experiments were performed for each concentration assessment of title compounds and each experiment was repeated twice.

Computational methods

All theoretical calculations were performed using the Jaguar 8.9 quantum program suite [28–31]. Single point and lowest-energy calculations were performed using Hartree–Fock theory and 6.31G** basic set. The crystal

structures were visualized and prepared for calculations using Maestro10.3 (Schrödinger) with MacroModel10.9 (Schrödinger). According to Koopmans's theorem [32] the energies of highest occupied (HOMO) and lowest (LUMO) unoccupied molecular orbitals were used to determine the ionization potential (I), and electron affinity (A) as in Eqs. (1) and (2). Accordingly, their derived parameters as band gap, electrophilicity (ω), hardness (η), chemical potential (μ), electronegativity (χ) and electrofelicity (ω) were calculated using Eqs. 3–6.

$$I \approx -\varepsilon_{HOMO} \quad (1)$$

$$A \approx -\varepsilon_{LUMO} \quad (2)$$

$$\eta \approx \frac{I - A}{2} \approx \frac{\varepsilon_{LUMO} - \varepsilon_{HOMO}}{2} \quad (3)$$

$$\mu \approx -\frac{I + A}{2} \approx \frac{\varepsilon_{LUMO} + \varepsilon_{HOMO}}{2} \quad (4)$$

$$\chi \approx \frac{I + A}{2} \approx \frac{-\varepsilon_{HOMO} - \varepsilon_{LUMO}}{2} \quad (5)$$

$$\omega = \frac{\mu^2}{2\eta} \quad (6)$$

Results and discussion

Synthesis and characterization

The title compounds 1–3 are stable in air at room temperature, and have been formed in accordance with the appropriate “rule of three” that serves as a guide for salt formation by determining the extent of proton transfer (Table 2). The principle of this rule is based on values of $\Delta\text{pK}_a = \text{pK}_a(\text{protonated base}) - \text{pK}_a(\text{acid})$ which is a tool for predicting salt or co-crystal formation. For values of ΔpK_a greater than 3 a molecular salt is formed, while for values less than 0 a co-crystal is formed [33]. For an intermediate value, no precise prediction can be

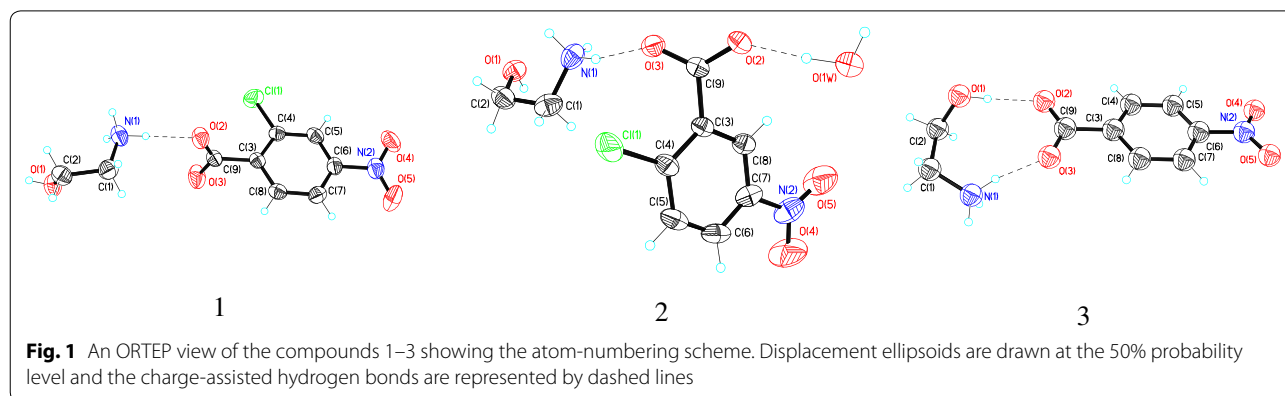


Table 1 Crystal data and structure refinement parameters for compounds 1–3

Compound	1	2	3 ^a
Empirical formula	C ₉ H ₁₁ ClN ₂ O ₅	C ₉ H ₁₃ ClN ₂ O ₆	C ₉ H ₁₂ N ₂ O ₅
Formula weight	262.65	280.66	228.21
Temperature (K)	293 (2)	293 (2)	293 (2)
Wavelength (Å)	1.54184	1.54184	0.71073
Crystal system	monoclinic	triclinic	monoclinic
Space group	<i>P</i> 2 ₁ / <i>c</i>	<i>P</i> -1	<i>P</i> 2 ₁ / <i>c</i>
Z	4	2	4
Unit cell dimensions			
<i>a</i> (Å)	8.402 (2)	7.019 (1)	6.211 (2)
<i>b</i> (Å)	6.334 (1)	9.512 (2)	8.651 (3)
<i>c</i> (Å)	22.023 (4)	9.740 (2)	19.594 (5)
α (°)	90	79.19 (3)	90
β (°)	100.72 (3)	88.58 (3)	91.27 (2)
γ (°)	90	78.42 (3)	90
<i>V</i> (Å ³)	1151.6 (4)	625.7 (2)	1052.6 (5)
<i>D</i> _{calc} (g cm ⁻³)	1.515	1.490	1.440
μ (mm ⁻¹)	3.099	2.950	0.119
<i>F</i> (000)	544	292	480
Crystal size (mm)	0.22 × 0.14 × 0.07	0.15 × 0.12 × 0.08	0.35 × 0.4 × 0.6
θ range for data collection (°)	4.09–70.07	4.62–70.01	2.08–27.06
Limiting indices	– 10 ≤ <i>h</i> ≤ 1 – 7 ≤ <i>k</i> ≤ 0 – 26 ≤ <i>l</i> ≤ 26	– 8 ≤ <i>h</i> ≤ 8 – 4 ≤ <i>k</i> ≤ 11 – 11 ≤ <i>l</i> ≤ 11	0 ≤ <i>h</i> ≤ 7 0 ≤ <i>k</i> ≤ 11 – 25 ≤ <i>l</i> ≤ 25
Reflections collected/unique	2336/2192	2370/2370	2501/2294
Reflections with [<i>I</i> > 2σ(<i>I</i>)]	2010	2282	1761
Parameters	156	165	193
Goodness-of-fit on <i>F</i> ²	1.007	1.003	1.001
<i>R</i> ₁ , <i>wR</i> ₂ [<i>I</i> > 2σ(<i>I</i>)]	0.0384, 0.1128	0.0415, 0.1175	0.0371, 0.1023
<i>R</i> ₁ , <i>wR</i> ₂ (all data)	0.0414, 0.1163	0.0424, 0.1187	0.0540, 0.11068
Largest difference in peak and hole (e Å ⁻³)	0.330/– 0.311	0.385/– 0.315	0.265/– 0.212

^a Crystallographic data of compound 3 [21] is presented here for comparison with compounds 1 and 2

made [34]. The melting points of compounds 1–3 are well defined, being lower than the corresponding acids (2-Cl-4-NO₂BA—m.p. 142 °C, 2-Cl-5-NO₂BA—m.p. 166 °C, 4-NO₂BA—m.p. 237 °C). The UV–vis spectral measurements indicate the cut off wavelength of 277.93, 279.81 nm, respectively 273.55 nm, and no characteristic absorptions in visible region were observed (Additional file 1: Figure S1).

The IR spectra provide the evidence of salt formation by the presence of absorption bands in the regions 1650–1540 and 1450–1360 cm⁻¹, arising from the asymmetric and symmetric vibrations of the COO⁻ group and by the absence of bands at 1710–1680 cm⁻¹, corresponding to carbonyl stretch (*v*_{C=O}) and 1320–1210 cm⁻¹ characteristic for *v*_{C–OH} vibrations in a COOH group (Additional file 1: Figure S2) [35, 36]. The appearance

of C–O vibrations at 1100–1000 cm⁻¹, belonging to –CH₂OH from EA was a supplementary proof of salt formation. The asymmetric –NH₃⁺ stretching vibrations are observed in the region 3200–2800 cm⁻¹ and weak bands of symmetric stretching –NH₃⁺ near 2600 and 2100 cm⁻¹. A strong –NH₃⁺ deformation band is observed at 1550–1485 cm⁻¹, which almost overlaps with asymmetric vibration of –NO₂ group at 1570–1485 cm⁻¹.

Crystal structure

The structural aspects of compounds 1 and 2 (Additional files 2 and 3) were investigated and compared with those of compound 3 [21]. X-ray study confirms that the proton transfer has occurred in both components, from the carboxyl group of acid to the amino group of ethanolamine, and the crystals are formed by two ionic species, anion

Table 2 Tabulated ΔpK_a and hydrogen-bonding geometry (\AA , $^\circ$) for compounds 1–3

ΔpK_a	D–H \cdots A	d(D–H)	d(H \cdots A)	d(D \cdots A)	(DHA)	Symmetry transformation for H-acceptor	
1	7.58	N(1)–H(2) \cdots O(2)	0.89	1.86	2.747 (2)	173	x, y, z
		N(1)–H(1) \cdots O(2)	0.89	2.12	2.815 (2)	135	$x + 1, y + 1, z + 1$
		N(1)–H(3) \cdots O(1)	0.89	2.20	2.868 (2)	131	$-x, -y + 1, -z + 1$
		O(1)–H(1) \cdots O(3)	0.82	1.87	2.681 (2)	169	$-x, -y + 1, -z + 1$
2	7.33	N(1)–H(1) \cdots O(3)	0.89	1.90	2.766 (2)	164	x, y, z
		N(1)–H(2) \cdots O(1)	0.89	1.96	2.798 (2)	156	$-x, -y, -z$
		N(1)–H(3) \cdots O(1W)	0.89	1.98	2.858 (2)	171	$-x + 1, -y, -z + 1$
		O(1)–H(1) \cdots O(3)	0.82	1.90	2.716 (2)	172	$x - 1, y, z$
		O(1W)–H(1) \cdots O(2)	0.97	1.99	2.857 (2)	149	$-x + 2, -y, -z + 1$
		O(1W)–H(2) \cdots O(2)	1.05	1.71	2.754 (2)	175	x, y, z
3^a	6.07	N(2)–H(2) \cdots O(1)	0.96	1.81	2.738	168	x, y, z
		O(5)–H(5) \cdots O(2)	0.87	1.81	2.683	177	x, y, z
		N(2)–H(2) \cdots O(5)	0.94	1.88	2.788	162	$-x - 1, +y - 1/2, -z + 1/2$
		N(2)–H(2) \cdots O(2)	0.94	1.81	2.757	170	$x + 1, y, z$

D and A are hydrogen bond donor and acceptor atoms. $\Delta pK_a = pK_a(\text{base}) - pK_a(\text{acid})$ were calculated using the pK_a data from Ref. [38]. All pK_a values have been determined in aqueous solutions

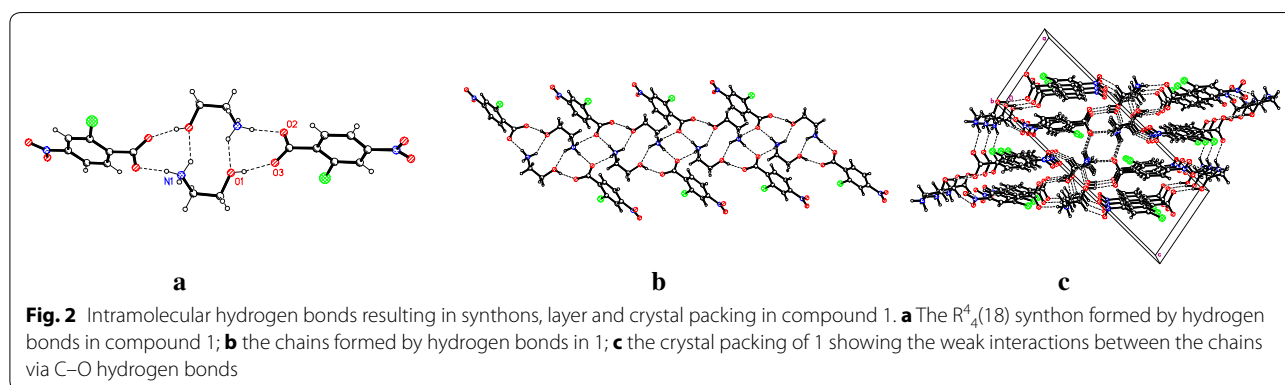
^a Data of compound 3 [21] are presented here for comparison with compounds 1 and 2

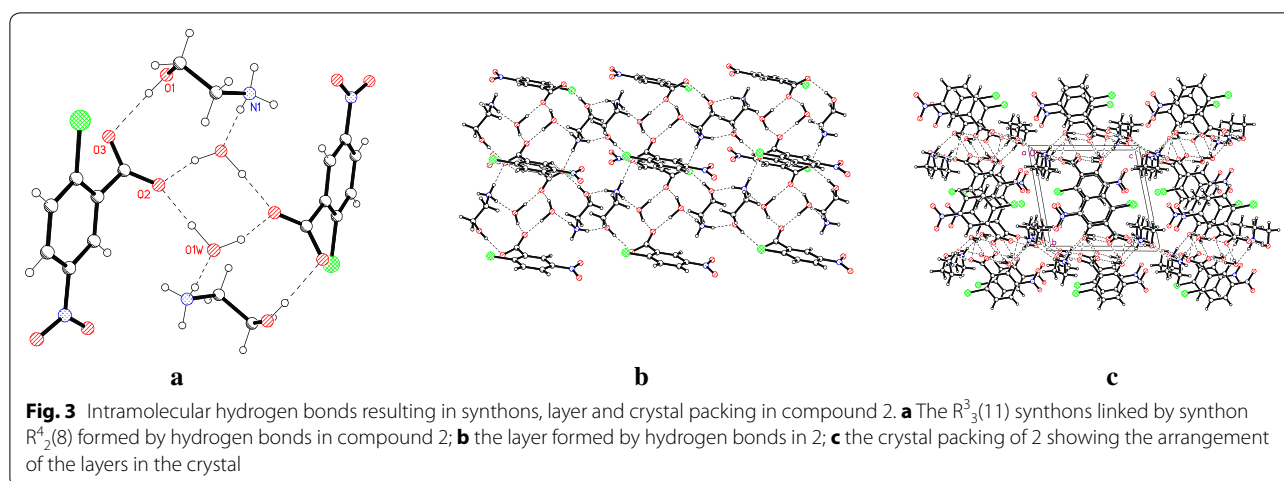
and cation. In chloronitro-compounds (1 and 2), the basic components are connected only by one hydrogen bond (HB) (Figs. 1, 2a, b, 3a, b and Table 2), while in nitro-compound (3) by two charged-assisted HB (Fig. 1). The ionic N–H \cdots O hydrogen bond plays the key role in formation of these pairs, being present in all investigated compounds. The geometric parameters for hydrogen bonds are given in Table 2. Bond lengths (\AA) and angles ($^\circ$) for compounds 1–3 are listed in Additional file 1: Table S1.

The anions in all compounds studied form a non-planar systems, more evident in compounds 1 and 2, where the dihedral angles between the least-square planes of the phenyl rings C(3)C(4)C(5)C(6)C(7)C(8) and the least-square planes of the $-\text{COO}^-$ and $-\text{NO}_2$ groups are

equal to 82.5 , 11.0° and 47.6 , 10.4° , while for compound 3 these values are 5.8 and 4.2° respectively. The cation adopts the—Syn-Clinal conformation, the N(1)C(1)C(2)O(1) torsion angles in compounds 1 and 2 being equal to -63.2° and 51.5° , respectively, towards compound 3 where is 77.4° .

In compound 1, the system of hydrogen bridges is formed only by the $-\text{NH}_3^+$ and $-\text{OH}$ groups from ethanolamine and carboxylate oxygen atoms. In this crystal, two cations and two anions are held together by two N–H \cdots O hydrogen bonds (N(1) \cdots O(2) $2.747(2)$ \AA) and two O–H \cdots O bonds (O(1) \cdots O(3) $2.682(2)$ \AA) (Fig. 2a). The $R^4_4(18)$ synthon is stabilized by two intermolecular hydrogen bonds N–H \cdots O (N(1) \cdots O(1) $2.868(2)$ \AA). These





synthons form infinite chains by four hydrogen bonds $N-H\cdots O$ ($N(1)\cdots O(2)$ 2.815(2) Å) (Fig. 2b), which are further consolidated into 2-D layers through $C-H\cdots O$ hydrogen bonds (where O is one oxygen atom from $-NO_2$ group of benzoate) developed along y direction (Fig. 2c). It is notable that a chlorine atom and the other oxygen atom from the NO_2 -group of benzoate are not involved in the crystalline structure.

Compound 2 differs from compound 1 by the position of the substituent atoms, and this compound crystallizes as a hydrate, which changes the system of hydrogen bonds (Table 2). Thus, in addition to the system of hydrogen bonds formed by the $-NH_3^+$ and $-OH$ groups from ethanolamine and carboxylate oxygen atoms, a water molecule is involved (Fig. 1). Water molecule acts as donor in the hydrogen bond with anion and as acceptor in hydrogen bond with cation. So, the nets contain $R^3_3(11)$ synthons formed by three hydrogen bonds ($N(1)\cdots O(1W)$ 2.858(2) Å, $O(1)\cdots O(3)$ 2.716(2) Å and $O(1W)\cdots O(2)$ 2.754(2) Å) linked between them by the $R^4_2(8)$ synthons formed by two $O-H\cdots O$ bonds ($O(1W)\cdots O(2)$ 2.754(2) Å and $O(1W)\cdots O(2)$ 2.857(2) Å). The cations, anions, and water molecules form hydrogen bonded chains, which are further hydrogen bonded to one another by pairs of water molecules, to form layers (Fig. 3a, b). The layers formed in this way stack along the y axis (Fig. 3c).

In the crystal structure of compound 3, the anion and cation are held together by two charge-assisted hydrogen bonds and form the infinite helix-like chains along b direction [21]. These chains are joined by glide plane in double chains through the $C(1)-H\cdots O(5)$ H-bonds (check labeling). Thus in the crystal packing of compounds 1 and 2, the anions and cations are self-assembled via $N-H\cdots O$, $O-H\cdots O$ hydrogen bonds to form the chains. These ones are consolidated into 2-D layers by $C-H\cdots O$ H-bonds and

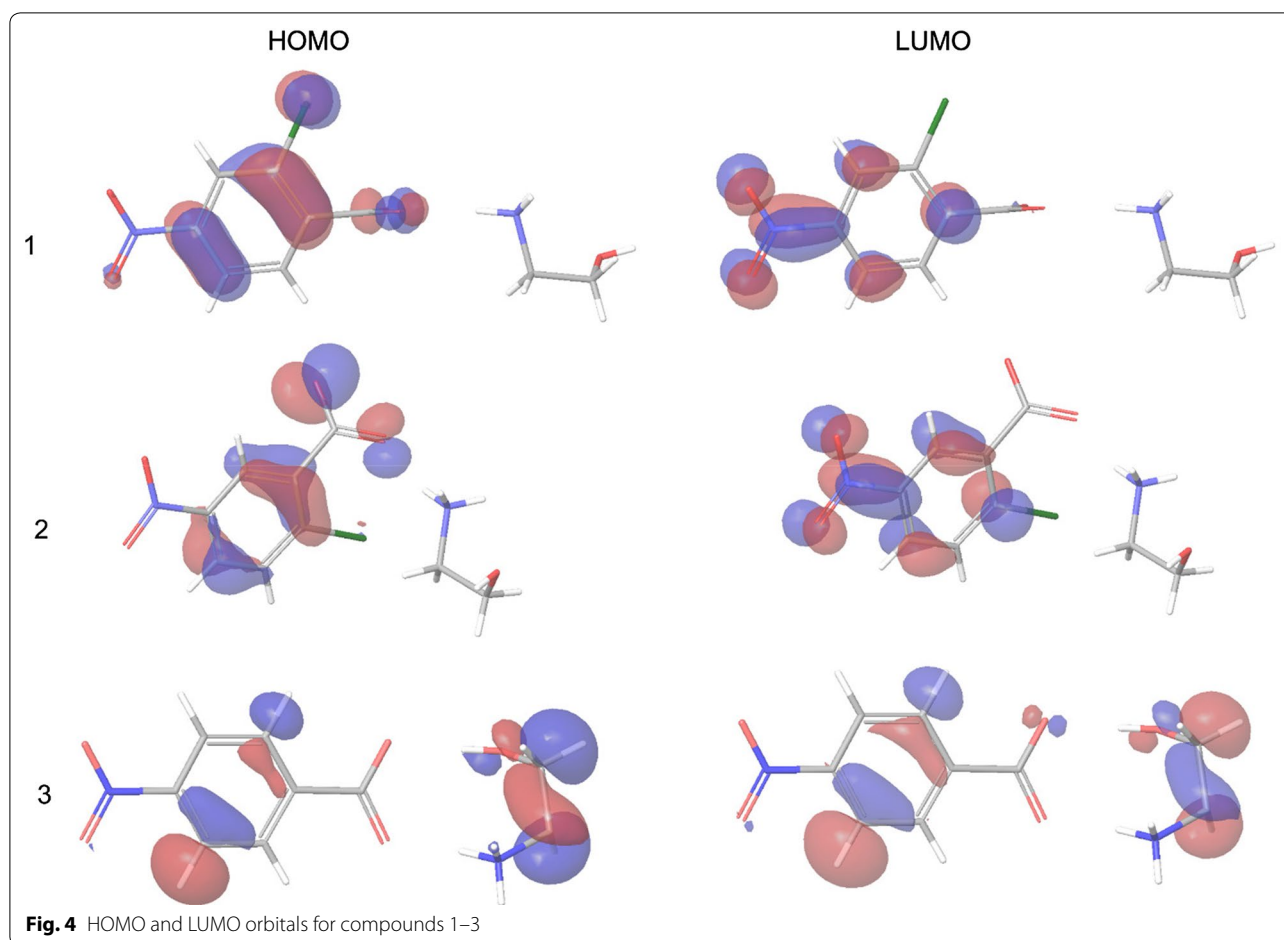
water molecules respectively, while the crystal packing of three adopts the chain-like structure. The anions in compounds 1 and 2 form essentially non-planar systems in comparison with that in compound 3.

Experimental determination and theoretical investigation of toxicity behaviour

The influence of the compounds studied against the transformation from larva to polyp of marine organism *H. echinata* was evaluated. The measured values of toxicity were found to be 3.22 logarithm unites (log u.), respectively 3.10 log u. in the case of chloronitro-compounds (1, 2) and 1.78 log u. for nitro-compound (3). This situation is of particular interest, because compound 3 shows a much lower toxicity (1.78 log u.) even if compared to individual components (4- NO_2 BA: 3.11 log u. and EA: 2.67 log u.).

With this purpose we proceed to investigate the molecular structures of the three compounds using ab initio methods given that the quantum chemical descriptors have shown good correlations with biological activity since the later is dependent on the nature of the compound. Using the frontier orbitals values, the energy gap and several global reactivity descriptors, such as chemical hardness (η), chemical potential (μ), electronegativity (χ) and electrophilicity index (ω), were calculated to evaluate the chemical reactivity and the stability of these compounds in order to elucidate a possible mechanism of action for this type of compounds.

The locations and values of HOMO and LUMO orbitals (Fig. 4) offer important evidences about the capability of a molecule to donate or to attract electrons. Compounds 1 and 2 have both first HOMO and LUMO orbitals distributed only on the anion. Compound 3 has a higher HOMO energy value which corresponds to a stronger electron-donating capacity, therefore to a higher reactivity.



The energy gaps between HOMO and LUMO orbitals (Additional file 1: Figure S3) offer information about chemical reactivity of a molecule, a small gap suggesting an easy electronic transition and therefore a higher chemical reactivity. Chloronitro-compounds 1 and 2 have a larger energy gap than nitro-compound 3, which means that the electron transfer between the HOMO and LUMO orbitals is more possible to occur in the case of compound 3 than in the case of compounds 1 and 2.

In the same manner, by analyzing the variation of other descriptors of reactivity (Table 3) compound 3 seems to exhibit a higher reactivity since it has the highest electronegativity number (highest electron

attraction tendency of molecules), the lowest chemical potential value (lowest escaping tendency of the electrons) and the highest electrophilicity index (highest electrophilic behavior) compared to its chlorinated derivatives.

When the descriptors illustrating the chemical stability were analysed (Table 4), we noticed that the chloro-derivatives had a more negative value for the heat of formation and a lower dipole moment value, which indicates a higher stability compared with compound 3. Compound 3 also has a lower hardness value than its chlorinated derivatives which makes it more susceptible to charge transfer and therefore more reactive. The chemical stability is usually associated to hard molecules.

Table 3 Chemical reactivity descriptors

Compound	Toxicity (logMRC50)	E_{HOMO} (eV)	E_{LUMO} (eV)	E_{gap} (eV)	μ (eV)	χ (eV)	ω (eV)
1	3.10	- 8.77077	2.20467	10.975	- 3.283	3.283	0.982
2	3.22	- 9.08751	1.61091	10.698	- 3.738	3.738	1.306
3	1.78	- 6.71305	- 4.72281	1.99	- 5.718	5.718	16.43

Table 4 Chemical stability descriptors

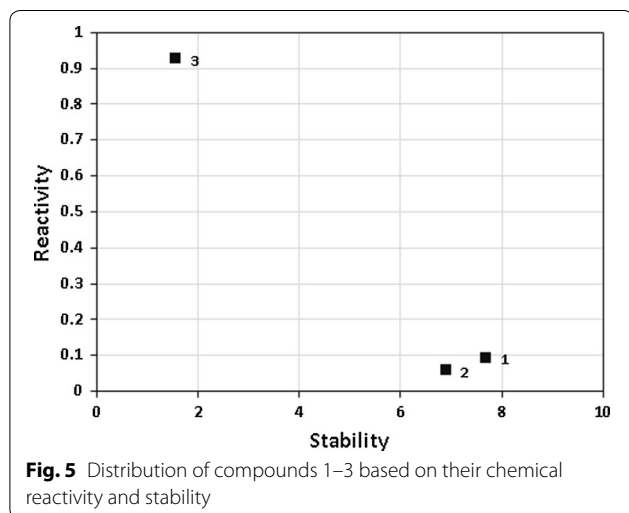
Compound	Toxicity (logMRC50)	Heat of formation (kcal mol ⁻¹)	Dipole	H (eV)
1	3.10	- 117.42	19.5258	5.488
2	3.22	- 121.19	17.5964	5.349
3	1.78	- 120.54	11.4651	0.995

We combined all the parameters describing the same characteristic of a molecule (reactivity or stability) in order to calculate a consensus score for each compound. We notice that compounds 1 and 2, which are more toxic, exhibit a higher stability and a lower reactivity (Fig. 5).

On the contrary, compound 3, which is less toxic, has a lower stability but a higher reactivity, although toxicity is usually associated with large values of reactivity [37]. In this light, probably the mechanism of action involves an accumulation of compounds 1 and 2 in the system since they do not react easily and are very stable.

Anion stability and reactivity

A similar trend in chemical reactivity and stability variation was noticed if only the anions were considered (A1–A3), given that the same alkanolamine is present in all three compounds and the anion is the active component. Besides the quantum chemical descriptors which have already been discussed, the chemical reactivity and stability of an anion may be correlated with its nucleophilic character and acidic strength. A measure of the nucleophilicity of a molecule is the ionization potential. A higher value of ionization energy, as in the case of A2 and A3, shows a higher attraction between the electron and the nucleus, therefore a lower reactivity (Table 5). The anion stability also depends on electron delocalization and aromaticity.

**Table 5 Ionization potentials and acidic constants for anions A1–A3**

Anion	Ionization potential (eV)	pKa ^a
A1	5.578062	1.92
A2	5.337785	2.17
A3	4.475456	3.43

^a pKa of correspondent carboxylic acid [38]

The electron density of the anions is determined by the electronic effects of substituents, so indirectly, if an acid is stronger, its conjugate base (anion) is weaker and more stable. Anion A3 is less stable, since the pKa of its conjugate acid is higher [38]. All three anions contain a nitro group with a resonance effect – R, that decreases the electron density at the aromatic ring, and thus it increases its inductive effect against carboxyl group, which can free easily the proton. 4-NO₂BA and 2-Cl-4-NO₂BA are stronger acids compared to 2-Cl-5-NO₂BA due to the presence of nitro group in *para* position, which implies a greater closeness of the carboxyl group to the positive charge which occurs on the aromatic ring through conjugation with nitro group. If the positive charge is closer to the carboxyl, the electrons are shifted closer to the oxygen atom and the anion is more stable. Chlorine atom containing pairs of non-bonding electrons has a resonance effect + E against the aromatic ring, functioning as a strong electron donor. Implicitly, the – R effect of nitro group is mitigated by the presence of chlorine per core, so the anion of compound 3 is a stronger acid and therefore has greater stability than those with chlorine.

Conclusions

Biological active salts with ethanolammonium as cation and 2-chloro-4-nitro/2-chloro-5-nitrobenzoate or 4-nitrobenzoate as anion were structurally, chemically and toxicologically investigated. Single crystal X-ray diffraction confirmed the proton transfer and ionic hydrogen bonds formation between the components. Therefore, in compounds 1 and 2, the components are linked only by one HB, while in compound 3 two charge-assisted HB are formed. Chloronitro compounds (1 and 2) adopt layered structure and nitrocompound (3) chain-like structure. The presence of chlorine atom in benzene

rings has led to rotation of carboxyl groups with respect to this ring which forms the essentially non-planar anions of 1 and 2 in comparison with compound 3. The position of nitro-substituent leads to change in the system of hydrogen bonds between anion and cation in compound 2 which crystallizes as hydrate. The measured value of toxicity indicates a very low order of toxicity for compound 3 (1.78 log u.), almost half of the value of compound 1, respectively 2 (3.22 log u., 3.10 log u.) and lower compared to the individual components (4-NO₂BA: 3.11 log u. and EA: 2.67 log u.). The theoretical study regarding chemical reactivity and stability profiles explains the experimental values of toxicity. Compound 3 showed a higher reactivity and a lower stability compared to its compound 1 and 2, which is in agreement with the lowest toxicity value measured in biological assay. In conclusion, toxicity test on *H. echinata* in relation with density functional theory, ab initio molecular orbital calculations and crystallographic study leads to a better understanding of nitro/chloronitro substituent effect on toxicity, contributing to the design of new compounds with low toxicity and practical applicability.

Additional files

Additional file 1. Additional information includes UV-vis spectra, FT-IR spectra, selected bond lengths (Å) and angles (°), the difference between HOMO and LUMO energies.

Additional file 2. Cif file for compound 1.

Additional file 3. Cif file for compound 2.

Authors' contributions

MC performed the synthesis and characterization of the compounds. LH realized the theoretical calculations. YC and PB did the crystallographic studies. SAC performed the toxicity test. All authors have contribution in write-up. All authors read and approved the final manuscript.

Author details

¹ Institute of Chemistry, Timisoara of Romanian Academy, 24 Mihai Viteazul Avenue, 300223 Timisoara, Romania. ² Institute of Applied Physics, Academy of Sciences of Moldova, Academiei Street 5, 2028 Chisinau, Republic of Moldova. ³ Siegstr. 4, 50859 Cologne, Germany.

Acknowledgements

This work was developed through a bilateral project between Romania and Moldova, CCCDI-UEFISCDI, PN3-P3-217/24BM/19.09.2016 (Romania), 16.80013.5007.04/RO (Moldova).

Competing interests

The authors declare that they have no competing interests.

Ethics approval and consent to participate

No human subjects are involved in this research.

Publisher's Note

Springer Nature remains neutral with regard to jurisdictional claims in published maps and institutional affiliations.

Received: 25 April 2017 Accepted: 10 November 2017

Published online: 06 December 2017

References

- Ono N (2002) The nitro group in organic synthesis. Wiley, New York
- Tripathi KD (2009) Essentials of medical pharmacology. Jaypee Brothers Medical Publishers (P) Ltd, New Delhi
- Zaragoza DF (2012) Nitro compounds. Wiley-VCH Verlag GmbH & Co, Weinheim
- Truong DD (2009) Tolcapone: review of its pharmacology and use as adjunctive therapy in patients with Parkinson's disease. *Clin Interv Aging* 4:109–113
- Raether W, Hanel H (2003) Nitroheterocyclic drugs with broad spectrum activity. *Parasitol Res* 90(Suppl 1):19–39
- Wilkinson SR, Christopher B, John MK, Belinda SH (2011) Trypanocidal activity of nitroaromatic prodrugs: current treatments and future perspectives. *Curr Top Med Chem* 11:2072–2084
- Singla D, Tewari R, Kumar A, Raghava G et al (2013) Designing of inhibitors against drug tolerant *Mycobacterium tuberculosis* (H37Rv). *Chem Cent J* 7:49
- Shakoor S, Ahsan T, Jabeen K, Raza M, Hasan R (2010) Use of p-nitrobenzoic acid in 7H10 agar for identification of *Mycobacterium tuberculosis* complex: a field study. *Int J Tuberc Lung Dis* 14:1644–1646
- Giampaglia CMS, Martins MC, Chimara E, Oliveira RS, de Oliveira Vieira GB et al (2007) Differentiation of *Mycobacterium tuberculosis* from other mycobacteria with p-nitrobenzoic acid using MGIT960. *Int J Tuberc Lung Dis* 11:803–807
- Kinchington D, Ng T, Mathews N, Tisdale M, Devine D, Ayuko WO (1997) Tcell costimulation by derivatives of benzoic acid. *Antivir Chem Chemother* 8:121–130
- Lemmerer A (2012) Covalent assistance to supramolecular synthesis: modifying the drug functionality of the antituberculosis API isoniazid in situ during co-crystallization with GRAS and API compounds. *Cryst-EngComm* 14:2465–2478
- Chicu SA, Grozav M, Kurunczi L, Crisan M (2008) SAR for amine salts of carboxylic acids to *Hydractinia echinata*. *Rev Chim* 59:582–587
- Isayev O, Rasulev B, Gorb L, Leszczynski J (2006) Structure-toxicity relationships of nitroaromatic compounds. *Mol Divers* 10:233–245
- Keshavarz MH, Pouretedal HR (2013) Simple and reliable prediction of toxicological activities of benzoic acid derivatives without using any experimental data or computer codes. *Med Chem Res* 22:1238–1257
- Sun Y, Li Z, Yan X, Wang L, Meng F (2009) Study on the quantitative structure–toxicity relationships of benzoic acid derivatives in rats via oral LD50. *Med Chem Res* 18:712–724
- Hemamalini M, Loh WS, Quah CK, Fun HK (2014) Investigation of supramolecular synthons and structural characterisation of aminopyridine-carboxylic acid derivatives. *Chem Cent J* 8:31
- Chen Z, Peng M (2011) Supramolecular architectures constructed from piperazine and substituted benzoic acids. *J Chem Crystallogr* 41:137–142
- Ishida H, Rahman B, Kashino S (2001) Morpholinium 2-chloro-4-nitrobenzoate, 2-chloro-5-nitrobenzoate and 4-chloro-3-nitrobenzoate. *Acta Crystallogr Sect C Cryst Struct Commun* 57:1450–1453
- Gibellini F, Smith TK (2010) The Kennedy pathway—de novo synthesis of phosphatidylethanolamine and phosphatidylcholine. *IUBMB Life* 62:414–428
- Rockenfeller P, Koska M, Pietroccola F, Minois N, Knittelfelder O et al (2015) Phosphatidylethanolamine positively regulates autophagy and longevity. *Cell Death Differ* 22:499–508
- Chumakov Y, Simonov Y, Grozav M, Bocelli G et al (2006) Hydrogen-bonding network in the organic salts of 4-nitrobenzoic acid. *Cent Eur J Chem* 4:458–475
- Crisan M, Bourosh P, Chumakov Y, Petric M, Ilia G (2013) Supramolecular assembly and Ab initio quantum chemical calculations of 2-hydroxyethylammonium salts of para-substituted benzoic acids. *Cryst Growth Des* 13:143–154

23. Crisan ME, Bourosh P, Maffei ME, Forni A, Pieraccini S, Sironi M, Chumakov YM (2014) Synthesis, crystal structure and biological activity of 2-hydroxyethylammonium salt of *p*-aminobenzoic acid. *PLoS ONE* 9:e101892
24. Chicu SA, Herrmann K, Berking S (2000) An approach to calculate the toxicity of simple organic molecules on the basis of QSAR analysis in *Hydractinia echinata* (Hydrozoa, Cnidaria). *Quant Struct Act Relat* 19:227–236
25. Dorosencu M, Rad R, Grozav M, Neamtii I (2001) The quantitative determination of some quaternary ammonium salts of benzoic acids. *Ann W U T-Ser Chem* 10:337–342
26. Sheldrick GM (1997) SHELX 97: programs for crystal structure analysis. University of Göttingen, Germany
27. Burnett MN, Johnson CK. ORTEP-III: Oak Ridge thermal ellipsoid plot program for crystal structure illustrations, Oak Ridge National Laboratory Report ORNL-6895, 1996
28. Bochevarov AD, Harder E, Hughes TF, Greenwood JR, Braden DA et al (2013) Jaguar: a high-performance quantum chemistry software program with strengths in life and materials sciences. *Int J Quantum Chem* 113:2110–2142
29. Schrödinger L (2015) New York, NY, Schrödinger Release 2015-3: Jaguar, 8.9 ed
30. Schrödinger L (2015) New York, NY, Schrödinger Release 2015-3: MacroModel, version 10.9 ed
31. Schrödinger L (2015) New York, NY, Schrödinger Release 2015-3: Maestro, version 10.3 ed
32. Koopmans T (1934) Über die Zuordnung von Wellenfunktionen und Eigenwerten zu den Einzelnen Elektronen Eines Atoms. *Physica* 1:104–113
33. Cruz-Cabeza AJ (2012) Acid-base crystalline complexes and the pKa rule. *CrystEngComm* 14:6362–6365
34. Delori A, Galek PTA, Pidcock E, Patni M, Jones W (2013) Knowledge-based hydrogen bond prediction and the synthesis of salts and cocrystals of the anti-malarial drug pyrimethamine with various drug and GRAS molecules. *CrystEngComm* 15:2916–2928
35. Pavia DL, Lampman GM, Kriz GS (2009) Introduction to spectroscopy: a guide for students of organic chemistry. W. B. Saunders Co., Philadelphia
36. Silverstein RM, Webster FX (1998) Spectrometric identification of organic compounds. Wiley, New York
37. Cronin MTD, Bajot F, Enoch SJ, Madden JC, Roberts DW, Schwöbel J (2009) The in chemico-in silico interface: challenges for integrating experimental and computational chemistry to identify toxicity. *ATLA* 37:513–521
38. Jover J, Bosque R, Sales J (2008) QSPR prediction of pKa for benzoic acids in different solvents. *QSAR Comb Sci* 27:563–581

Submit your manuscript to a SpringerOpen[®] journal and benefit from:

- Convenient online submission
- Rigorous peer review
- Open access: articles freely available online
- High visibility within the field
- Retaining the copyright to your article

Submit your next manuscript at ► springeropen.com
